Aerospace Science and Technology 47 (2015) 467–472

Contents lists available at ScienceDirect

Aerospace Science and Technology

www.elsevier.com/locate/aescte

Optimal redundant sensor configuration for accuracy increasing in space inertial navigation system

Mehdi Jafari [1]

KNTU University of Technology, Iran

ARTICLE INFO

Article history:
Received 11 June 2012
Received in revised form 2 October 2012
Accepted 18 September 2015
Available online 9 October 2015

Keywords:
Inertial navigation system
Optimal configuration
Redundant sensor
Accuracy increasing
Reliability

ABSTRACT

A redundant inertial measurement unit (IMU) is an inertial sensing device composed by more than three accelerometers and three gyroscopes. This paper analyzes the performance of redundant IMUs and their various sensors configurations. The inertial instruments can achieve high reliability for long periods of time only by redundancy. By suitable geometric configurations it is possible to extract the maximum amount of reliability and accuracy from a given number of redundant single-degree-of-freedom gyros or accelerometers. This paper gives general derivation of the optimum matrix which can be applied to the outputs of any combination of 3 or more sensors to obtain 3 orthogonal vector components based on their geometric configuration and error characteristics. Certain combinations of 4 or more instruments have the capability of detecting an instrument malfunction, those of 5 additional capabilities of isolating that malfunction to a particular sensor.

1. Introduction

The main purposes of the redundant sensors are to provide highly reliable and accurate sensor data and also reconfigure sensor network systems if some sensors failed. These create the fundamentals for the design of fault-tolerant navigation systems and the achievement of reliability and integrity of inertial navigation systems. Overall navigation improvement is to be expected as there is more input information. Through increased redundancy we can obtain noise reduction in the navigation output parameters.

The advantages of using multiple sensors over a single sensor to improve the accuracy of acquired information about an object have been recognized and employed by many engineering disciplines ranging from applications such as a medical decision-making aid system to a combined navigation system [3]. Weis and Allan presented a high-accuracy clock with a month error of one second through combining three inexpensive wrist watches with month errors of 40 seconds in 1992 [4]. Actually this technology used heterogeneous sensor data fusion to improve the accuracy. Recently, some researchers have begun to take the similar idea to improve the accuracy of sensor. Bayard combined four inexpensive gyroscopes to form a virtual sensor with higher accuracy output, and called this technology ‘virtual gyroscope’ [5]. In the virtual gyroscope the random noise of the gyroscope was estimated by using the Kalman filtering for the further compensation, thus its accuracy was improved.

The correlation between the sensors was used to establish the covariance matrix of the system random noise for filtering computation and better accuracy improvements. Lam proposed a very interesting concept to enhance the accuracy of sensors via dynamic random noise characterization and calibration [3,6,7]. The first compensation uses external aiding sensors data such as GPS sensors, thus the high noise drift errors such as bias, scale factor, and misalignment errors inherently existing in MEMS sensors will be eliminated. The second compensation uses signal isolation and stochastic model propagation to dynamically monitor changes and identify random noise parameters of MEMS inertial sensors such as angular random walk, angular white noise and rate random walk, etc. Through analyzing the current various multi-sensor fusion methods, we find that these approaches could be improved further in several ways for better accuracy improvements. In the virtual gyroscope, Bayard established the covariance matrices of process noises and measurement noises separately for the Kalman filtering.

1.1. Fault detection and isolation

Redundancy is on the basis of hypothesis testing for error detection and isolation. With redundant inertial measurements we can increase the reliability aspects at the IMU and detect defective sensors and unreal signals.

E-mail address: m_jaafari_h@yahoo.com.
[1] PHD of Aerospace Engineering.

http://dx.doi.org/10.1016/j.ast.2015.09.017

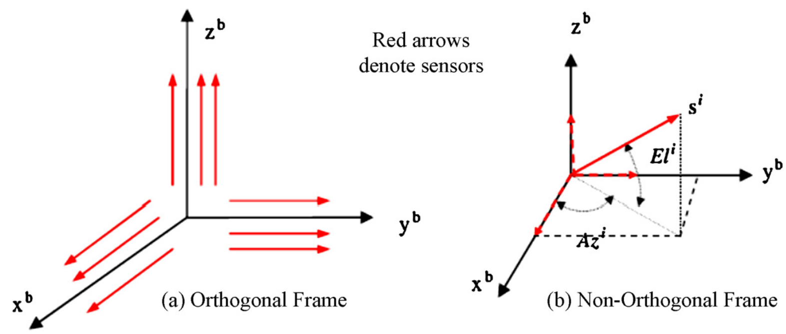

Fig. 1. Sensor installation orientation. (For interpretation of the references to color in this figure legend, the reader is referred to the web version of this article.)

The use of redundant IMUs for navigation purposes is not new. From the very early days of the inertial technology, the inertial navigation community was aware of the need and benefits of redundant information. However, the focus of the research and development efforts was fault detection and isolation (FDI). In the early days, the idea was to make use of the redundancy in order to support fault-safe systems. A fault-tolerant system is able not only to detect a defective sensor, but also to isolate it. After isolating a defective sensor, the system may keep working as a fault-tolerant or a fault-safe system depending on the number of remaining sensors. By means of voting schemes [9], it can be shown that a minimum of four sensors are needed to devise a fault-safe system and a minimum of five to devise a fault-isolation one. Sensor configuration for optimal state estimation and optimal FDI was, as well, a topic of research in the early works.

In [1,2] a comprehensive analysis of the optimal spatial configuration of sensors for FDI applications is provided together with FDI algorithms. In addition, the performance for fail-isolation systems in case a sensor is removed due to failure. More recent results on the use of redundant inertial sensors for FDI can be found in [10] and [8]. The former is mainly concerned with the use of skewed redundant configurations for unmanned air vehicles while the latter focuses in guidance, navigation and control of underwater vehicles. The two references are good examples of the wide range of applications for skewed redundant configurations that are currently under research.

1.2. Clustered sensor

Measurement information provided by various navigation sensor systems can be independent, redundant, complementary or cooperative. For example, gyroscope set and accelerometer set, each individually providing independent measurements, are integrated in an IMU to provide complementary and cooperative information that are used to derive the navigation states.

The clustered sensor has different configurations. Two approaches to the configuration of a redundant IMU system have been suggested in the past.

- One is an orthogonal configuration shown in Fig. 1(a) where the sensing axes of redundant inertial sensors are orthogonal or parallel with respect to the body axes. In the orthogonal configuration, the inertial measurement sensed by one sensor mounted on one axis is independent of other measurements sensed by other sensors mounted on other axes. Therefore, the orthogonal IMU measurements are decoupled along the orthogonal axes.
- The other uses a non-orthogonal configuration relative to the body axes shown in Fig. 1(b), referred to as skewed redundant IMU (SRIMU) configurations. In a non-orthogonal configuration, the measurement sensed by one sensor can be decomposed into three components along the orthogonal axes, red dash arrows shown in Fig. 1(b). Therefore, the measured states are coupled with each other in the SRIMU measurements. This nature allows fewer sensors to be used in an SRIMU configuration in order to achieve system performance equivalent to the orthogonal IMU system.

Table 1
Polyhedrons in redundant sensor configurations.

Polyhedron	Number of faces	Min number of sensors for redundancy
Cube	6	≥4
Cone (Pyramid)	≥4	≥4
Dodecahedron	12	6

Although the orthogonal IMU system is a conventional configuration, it is not the most efficient way to exploit the benefits of redundant sensor systems in a fault-tolerant navigation system. The orthogonal configuration has been used in traditional fault-tolerant navigation systems.

SRIMU systems can most effectively make use of redundant measurements provided by multiple sensors and have various configuration geometries dependent on the number of sensors. The typical configuration geometries are based on regular polyhedrons in order to simplify the engineering implementation. Several geometries commonly used in redundant sensor configurations are summarized in Table 1.

2. Optimal configuration of inertial redundant sensor system

Redundancy can be provided by installing a few independent, identical copies of a system and comparing their outputs. Inertial navigation systems are often used in threes, and a computer correlates their outputs. If two of the three consistently differ from the third, the third is considered to have failed and its data is ignored. Deciding between two might be possible if other data from separate sensors are available.

Redundant systems are expensive; the cost of providing backup systems must include the cost of carrying their-extra weight. Rather than installing three copies of a system, redundancy can be provided at the component level.

Particular system designs include one in which a fourth single-axis sensor is mounted with its sensitive axis skewed to the three basic sensor axes. This sensor can then act as a check on the basic three and can provide information if one should be determined to have failed.

2.1. Criteria for optimal SRIMU configurations

In an SRIMU (Sensors Redundant IMU) configuration, the orientation of each sensor axis is defined by its azimuth and elevation angles with respect to an orthogonal reference frame, such as the body frame.

Let each axis of the instrument frame be presented by a unit vector $\mathbf{S^i}$ along the sensing direction of sensor i, the unit vector can be defined in the orthogonal reference frame by:

$$S^i = \cos(El^i)\cos(Az^i).\mathbf{i} + \cos(El^i)\sin(Az^i).\mathbf{j} + \sin(El^i).\mathbf{k} \tag{2.1}$$

where:

- ✓ The bold symbols **i**, **j** and **k** are three unit vectors along the corresponding axes of the reference frame (x^b, y^b, z^b).
- ✓ The superscript i denotes a sensor and its sensing axis.
- ✓ $\mathbf{El^i}$ and $\mathbf{Az^i}$ are the elevation and azimuth angles of the instrument axis i with respect to the reference frame.

If we suppose that an SRIMU system encloses n sensors, identified by $1, 2, 3, \ldots, n$, the measurement equations of the SRIMU system can be formulated as follows:

$$\begin{bmatrix} m_1 \\ m_2 \\ \vdots \\ m_n \end{bmatrix} = \begin{bmatrix} i.S^1 & j.S^1 & k.S^1 \\ i.S^2 & j.S^2 & k.S^2 \\ \vdots & \vdots & \vdots \\ i.S^n & j.S^n & k.S^n \end{bmatrix} \begin{bmatrix} w_x \\ w_y \\ w_z \end{bmatrix} + \begin{bmatrix} v_1 \\ v_2 \\ \vdots \\ v_n \end{bmatrix} \tag{2.2}$$

or in vector form

$$m = H.w + v \tag{2.3}$$

where:

- ✓ w_x, w_y and w_z are three measured physical input quantities, such as accelerations or angular rates in the body frame.
- ✓ m_i is the measurement of sensor i.
- ✓ v_i is the measurement error, witch is a Gaussian white noise with a zero-mean value and standard deviation σ_i.
- ✓ H is known as the sensor geometry matrix, or design matrix and describes the configuration of an SRIMU system.
- ✓ The symbol (.) presents the operation of dot product of two vectors.

In essence, H matrix defines the geometrical arrangement of the sensors with respect to the orthogonal body frame. The matrix formulation is same for accelerometer or gyro.

2.2. Covariance matrix

Applying a weighted least-squares estimator, the estimate of the measured state vector $\hat{w}$ is given by:

$$\hat{w} = (H^T W H)^{-1} H^T W m = C^b_{\text{instru}} m \tag{2.4}$$

where W is the weight matrix and C^b_{instru} is referred to as the transformation matrix from the inertial instrument frame to the body frame. Defining the estimate error vector $\tilde{w} = w - \hat{w}$ then:

$$\begin{aligned} \tilde{w} &= w - \hat{w} = w - (H^T W H)^{-1} H^T W m \\ &= w - (H^T W H)^{-1} H^T W (Hw + v) \\ &= -(H^T W H)^{-1} H^T W v \end{aligned} \tag{2.5}$$

Therefore, the estimate error is the normal distribution and the covariance matrix of the estimate errors according to the covariance transfer law is given by:

$$\begin{aligned} \text{Var}(\tilde{w}) &= E\left[(w - \hat{w})(w - \hat{w})^T\right] \\ &= (H^T W H)^{-1} H^T W R W H^T (H^T W H)^{-1} \end{aligned} \tag{2.6}$$

where:

- ✓ $R = \text{Var}(v v^T)$ is the noise covariance matrix.

To simplify the analysis of performance of an SRIMU configuration, assume that all of sensor noises are independent and that the standard deviation of the noise for each sensor measurement is identical σ_v, and if the weight matrix W is taken as the inverse of R, then the covariance matrix of the estimate error becomes

$$\text{Var}(\tilde{w}) = (H^T R^{-1} H)^{-1} = \sigma_v^2 (H^T H)^{-1} \tag{2.7}$$

or is represented by the following normalized form

$$\sigma_{\tilde{w}}^2 = \frac{\text{Var}(\tilde{w})}{\sigma_v^2} = (H^T H)^{-1} \tag{2.8}$$

The probability density function of the estimate error can be given by

$$f_{\tilde{w}}(X) = \frac{1}{(\sqrt{2\pi})^3 \sqrt{|\sigma_{\tilde{w}}^2|}} \exp\left(-\frac{X^T X}{2\sigma_{\tilde{w}}^2}\right) \tag{2.9}$$

Then, the locus of the point X is determined by

$$\frac{X^T X}{\sigma_{\tilde{w}}^2} = K \tag{2.10}$$

This represents an error ellipsoid with a surface of constant likelihood. For any K, the volume of this ellipsoid is given by

$$V = \frac{4}{3}(\sqrt{K})^3 \pi \sqrt{|\sigma_{\tilde{w}}^2|} \tag{2.11}$$

From the analysis above, the smaller the volume of this ellipsoid, the smaller the estimate errors, and the performance of navigation systems with various SRIMU.

Configurations can be determined by $\sqrt{|\sigma_{\tilde{w}}^2|}$.

2.3. Determination of the optimal azimuth and elevation angles

Define a performance index (PI) as:

$$\text{PI} = \sqrt{|\sigma_{\tilde{w}}^2|} = \sqrt{\det(H^T H)^{-1}} \tag{2.12}$$

This equation can be used to determine the azimuth and elevation angles of each sensor to construct an optimal SRIMU configuration.

2.4. The criterion of minimum GDOP

If the square root of the trace of the normalized covariance matrix is selected as a criterion to optimize an SRIMU configuration, known as the geometric dilution of precision (GDOP), then

$$\text{GDOP} = \sqrt{\text{tr}(H^T H)^{-1}} \tag{2.13}$$

We use the criterion of minimum GDOP to analyze the optimal installation angles for several cone configurations. However, this criterion cannot be applied to non-cone SRIMU configurations.

2.5. The optimal performance of non-cone SRIMU configurations

To evaluate the optimal performance of non-cone SRIMU configurations, the estimate error variances of the measured states in the body frame from Eq. (2.4) can be formulated as follows.

$$\sigma_w^2(i) = \sum_{j=1}^{n} C^b_{\text{instru}}(i, j)^2 \sigma_j^2, \quad i = x, y, z \tag{2.14}$$

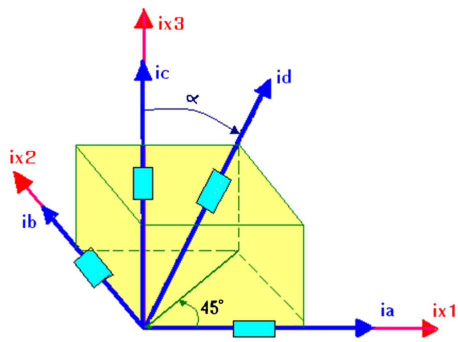

Fig. 2. Four-sensors cube configuration.

Based on the assumption that all measurement noises have an identical variance $\sigma_v^2 = \sigma_j^2$ a normalized error variance is given by

$$\sigma_N^2(i) = \frac{\sigma_w^2(i)}{\sigma_v^2} = \sum_{j=1}^{n} C^b_{\text{instru}}(i, j)^2, \quad i = x, y, z \tag{2.15}$$

where $C^b_{\text{instru}}(i, j)$ is the corresponding element of C^b_{instru} accordingly.

The criterion for determining the optimal SRIMU installation angles is based on the allocation of the uncertainty of SRIMU measurement to three orthogonal reference axes, usually the body axes. For example, to precisely sense aircraft motion along a specific body-axis direction, the criterion for minimizing the corresponding $\sigma_N^2(i)$ can be used to determine the SRIMU installation angles. To allocate the uncertainty of SRIMU measurement equally to three body axes, then the following criteria

$$\sigma_N(x) = \sigma_N(y) = \sigma_N(z) \tag{2.16}$$

can be selected to determine the SRIMU installation angles.

2.6. Four-sensors configuration

Four-sensors cube configuration: The Fig. 2 shows this configuration. From the above figure we can find the following equations:

$$i_a.i_{x1} = 1$$

$$i_b.i_{x2} = 1$$

$$i_c.i_{x3} = 1$$

$$i_d.i_{x3} = \cos(\alpha)$$

$$i_d.i_{x1} = i_d.i_{x2} = \frac{\sqrt{2}}{2}\sin(\alpha)$$

So the relation between the redundant sensors and the body frame can be written as:

$$\begin{bmatrix} i_a \\ i_b \\ i_c \\ i_d \end{bmatrix} = \begin{bmatrix} 1 & 0 & 0 \\ 0 & 1 & 0 \\ 0 & 0 & 1 \\ \frac{\sqrt{2}}{2}\sin(\alpha) & \frac{\sqrt{2}}{2}\sin(\alpha) & \cos(\alpha) \end{bmatrix} . \begin{bmatrix} i_{x1} \\ i_{x2} \\ i_{x3} \end{bmatrix}$$

Therefore, the measurements matrix for the Four-Sensors Cube configuration is:

$$H_{4\text{-cube}} = \begin{bmatrix} 1 & 0 & 0 \\ 0 & 1 & 0 \\ 0 & 0 & 1 \\ \frac{\sqrt{2}}{2}\sin(\alpha) & \frac{\sqrt{2}}{2}\sin(\alpha) & \cos(\alpha) \end{bmatrix}$$

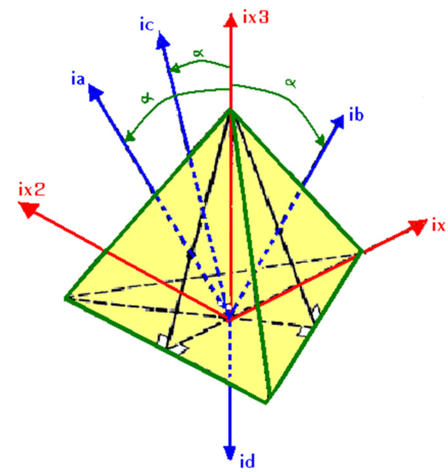

Fig. 3. Four-sensors cone with one axis cone sensor configuration.

The optimal angle for this configuration is:

$$\sin^2(\alpha) = \frac{2}{3} \quad \Rightarrow \quad \alpha = 54.7356^\circ$$

The matrix that relates the output sensors to the body axes when all sensors operating properly is given by

$$B = \left(H^T H\right)^{-1} H^T = \begin{bmatrix} 0.8333 & -0.1667 & -0.1667 & 0.2887 \\ -0.1667 & 0.8333 & -0.1667 & 0.2887 \\ -0.1667 & -0.1667 & 0.8333 & 0.2887 \end{bmatrix}$$

Four-sensor cone with one axis cone sensor configuration: The Fig. 3 shows this configuration. From the above figure we can find the following equations:

$$i_a.i_{x3} = i_b.i_{x3} = i_c.i_{x3} = \cos(\alpha)$$

$$i_d = -i_{x3}$$

$$i_a.i_{x1} = -\sin(\alpha)$$

$$i_b.i_{x1} = i_c.i_{x1} = \frac{1}{2}\sin(\alpha)$$

$$i_b.i_{x2} = i_c.i_{x2} = -\frac{\sqrt{3}}{2}\sin(\alpha)$$

So the relation between the redundant sensors and the body frame can be written as:

$$\begin{bmatrix} i_a \\ i_b \\ i_c \\ i_d \end{bmatrix} = \begin{bmatrix} -\sin(\alpha) & 0 & \cos(\alpha) \\ \frac{1}{2}\sin(\alpha) & -\frac{\sqrt{3}}{2}\sin(\alpha) & \cos(\alpha) \\ \frac{1}{2}\sin(\alpha) & \frac{\sqrt{3}}{2}\sin(\alpha) & \cos(\alpha) \\ 0 & 0 & -1 \end{bmatrix} . \begin{bmatrix} i_{x1} \\ i_{x2} \\ i_{x3} \end{bmatrix}$$

The optimal angle for this configuration is:

$$\sin^2(\alpha) = \frac{8}{9} \quad \Rightarrow \quad \alpha = 70.5288^\circ$$

The matrix that relates the output sensors to the body axes when all sensors operating properly is given by

$$\mathrm{B} = \left(H^T H\right)^{-1} H^T = \begin{bmatrix} -0.7071 & 0.3536 & 0.3536 & 0 \\ 0 & -0.6124 & 0.6124 & 0 \\ 0.25 & 0.25 & 0.25 & -0.75 \end{bmatrix}$$

Four-sensors cone configuration without one axis cone sensor: The most symmetric configuration of four sensors input axes is the normal to the faces of a regular tetrahedron. The Fig. 4 shows this configuration. From the above figure we can find the following equations:

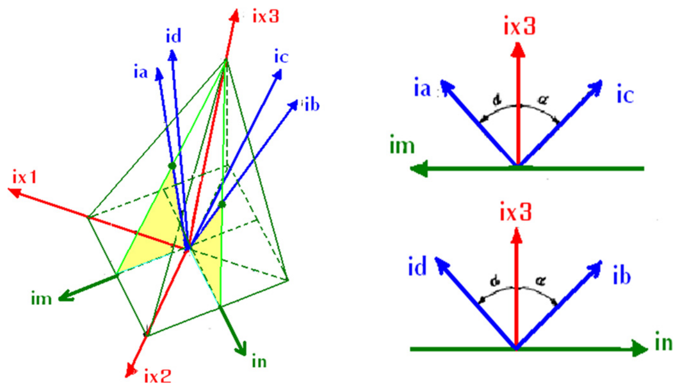

Fig. 4. Four-sensors cone without one axis cone sensor configuration.

$$i_a.i_b = i_b.i_c = i_c.i_d = i_d.i_a = 0$$

$$i_a.i_{x3} = i_b.i_{x3} = i_c.i_{x3} = i_d.i_{x3} = \cos(\alpha)$$

$$i_a.i_{x1} = i_a.i_{x2} = i_b.i_{x3} = i_d.i_{x1} = \frac{\sqrt{2}}{2}\sin(\alpha)$$

$$i_b.i_{x1} = i_c.i_{x1} = i_c.i_{x2} = i_d.i_{x2} = -\frac{\sqrt{2}}{2}\sin(\alpha)$$

So the relation between the redundant sensors and the body frame can be written as:

$$\begin{bmatrix} i_a \\ i_b \\ i_c \\ i_d \end{bmatrix} = \begin{bmatrix} \frac{\sqrt{2}}{2}\sin(\alpha) & \frac{\sqrt{2}}{2}\sin(\alpha) & \cos(\alpha) \\ -\frac{\sqrt{2}}{2}\sin(\alpha) & \frac{\sqrt{2}}{2}\sin(\alpha) & \cos(\alpha) \\ -\frac{\sqrt{2}}{2}\sin(\alpha) & -\frac{\sqrt{2}}{2}\sin(\alpha) & \cos(\alpha) \\ \frac{\sqrt{2}}{2}\sin(\alpha) & -\frac{\sqrt{2}}{2}\sin(\alpha) & \cos(\alpha) \end{bmatrix} \cdot \begin{bmatrix} i_{x1} \\ i_{x2} \\ i_{x3} \end{bmatrix}$$

The optimal angle for this configuration is:

$$\sin^2(\alpha) = \frac{2}{3} \quad \Rightarrow \quad \alpha = 54.7356^\circ$$

The matrix that relates the output sensors to the body axes when all sensors operating properly is given by

$$B = \left(H^T H\right)^{-1} H^T = \begin{bmatrix} 0.4330 & -0.4330 & -0.4330 & 0.4330 \\ 0.4330 & 0.4330 & -0.4330 & -0.4330 \\ 0.4330 & 0.4330 & 0.4330 & 0.4330 \end{bmatrix}$$

2.7. Six-sensors cone configuration

The Fig. 5 shows this configuration. From the above figure we can find the following equations:

$$i_a.i_{x3} = i_b.i_{x3} = i_c.i_{x3} = i_d.i_{x3} = i_e.i_{x3} = i_f.i_{x3} = \cos(\alpha)$$

$$i_a.i_{x1} = i_c.i_{x2} = i_e.i_{x3} = \sin(\alpha)$$

$$i_b.i_{x1} = i_d.i_{x2} = i_f.i_{x3} = -\sin(\alpha)$$

So the relation between the redundant sensors and the body frame can be written as:

Table 2
The comparison of the errors for different sensors configurations.

Number of sensors		Errors	
Total	Operating	GDOP	PI
Three-sensors orthogonal	3	1.7321	1
Four-sensors cube	4	1.5811	0.7071
	3	2.6458	1.7321
Four-sensors cone with one axis cone sensor	4	1.5000	0.6495
	3	2.1213	1.2990
Four-sensors cone without one axis cone sensor	4	1.5000	0.6495
	3	2.1213	1.2990
Five-sensors cone	5	1.3416	0.4648
	4	1.6432	0.7348
	3	3.0468	1.9767
Six-sensors cone	6	1.2247	0.3536
	5	1.4142	0.5000
	4	1.7321	0.7906
	3	2.0361	1.3143

$$\begin{bmatrix} i_a \\ i_b \\ i_c \\ i_d \\ i_e \\ i_f \end{bmatrix} = \begin{bmatrix} \sin(\alpha) & 0 & \cos(\alpha) \\ -\sin(\alpha) & 0 & \cos(\alpha) \\ \cos(\alpha) & \sin(\alpha) & 0 \\ \cos(\alpha) & -\sin(\alpha) & 0 \\ 0 & \cos(\alpha) & \sin(\alpha) \\ 0 & \cos(\alpha) & -\sin(\alpha) \end{bmatrix} \cdot \begin{bmatrix} i_{x1} \\ i_{x2} \\ i_{x3} \end{bmatrix}$$

The optimal angle for this configuration is:

$$\sin^2(\alpha) = \frac{2}{3} \quad \Rightarrow \quad \alpha = 54.7356^\circ$$

The matrix that relates the output sensors to the body axes when all sensors operating properly is given by

$$B = \left(H^T H\right)^{-1} H^T = \begin{bmatrix} 0.2629 & -0.2629 & 0.4253 & 0.4253 & 0 & 0 \\ 0 & 0 & 0.2629 & -0.2629 & 0.4253 & 0.4253 \\ 0.4253 & 0.4253 & 0 & 0 & 0.2629 & -0.2629 \end{bmatrix}$$

2.8. Error analysis

Based on the following equation:

$$\mathrm{PI} = \sqrt{\left|\sigma_{\tilde{w}}^2\right|} = \sqrt{\det\left(H^T H\right)^{-1}}$$

$$\mathrm{GDOP} = \sqrt{\mathrm{tr}\left(H^T H\right)^{-1}}$$

for the previous sensors configuration, the effective errors are given in Table 2 and below normalized to the error assuming of a conventional three-sensors unit is unity. Comparing the third and fourth columns of Table 2, if sensor failures occurred, optimal configurations may not obtain better measurement accuracy in comparison with a non-optimal configuration. Therefore, the selection of an SRIMU configuration is a tradeoff between failure detection performance and measurement accuracy under conditions of no sensor failures and sensor failures. Fig. 6 shows errors comparing for different sensors configuration in case of failure in one sensor and without any failure.

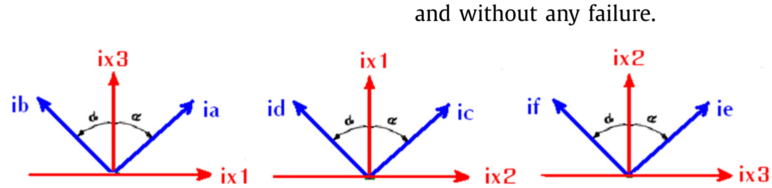

Fig. 5. Six-sensors cone configuration.

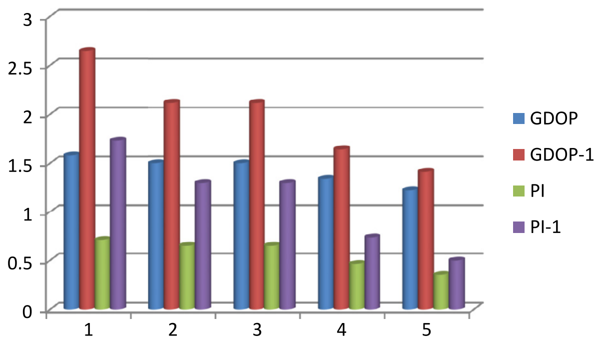

Fig. 6. Errors comparing for different sensors configuration. In case of failure in one sensor and without any failure.

3. Summary

In this paper, we analyze the performance of redundant IMUs and their various sensors configurations. This paper gives general derivation of the optimum matrix which can be applied to the outputs of any combination of 3 or more sensors to obtain 3 orthogonal vector components based on their geometric configuration and error characteristics. Comparing the third and fourth columns of Table 2, if sensor failures occurred, optimal configurations may not obtain better measurement accuracy in comparison with a non-optimal configuration. Therefore, the selection of an SRIMU configuration is a tradeoff between failure detection performance and measurement accuracy under conditions of no sensor failures and sensor failures.

Conflict of interest statement

None declared.

References

[1] M. Sturza, Navigation systems integrity monitoring using redundant measurements, Navigation 35 (4) (1988) 69–87.
[2] M. Sturza, Skewed axis inertial sensor geometry for optimal performance, in: AIAA/IEEE Digital Avionics Systems Conference, 1988, pp. 128–135.
[3] Q.M. Lam, T. Wilson Jr., R. Contillo, D. Buck, Enhancing MEMS sensors accuracy via random noise characterization and calibration, Proc. SPIE 5403 (2004) 427–438.
[4] M. Weis, D. Allan, Smart clock: a new time, IEEE Trans. Instrum. Meas. 41 (1992) 915–918.
[5] D.S. Bayard, S.R. Ploen, High accuracy inertial sensors from inexpensive components, US Patent US20030187623A1, 2003.
[6] Q.M. Lam, N. Stamatakos, C. Woodruff, S. Ashton, Gyro modeling and estimation of its random noise sources, in: AIAA Guidance, Navigation, and Control Conference and Exhibit, Austin, Texas, vol. 5562, 2003, pp. 1–11.
[7] Q.M. Lam, T. Hunt, P. Sanneman, S. Underwood, Analysis and design of a fifteen state stellar inertial attitude determination system, in: AIAA Guidance, Navigation, and Control Conference and Exhibit, Austin, Texas, vol. 5483, 2003, pp. 11–14.
[8] A. Lennartsson, D. Skoogh, Sensor redundancy for inertial navigation, Technical report, FOI (Swedish Defence Research Agency), SE, 2003.
[9] A. Pejsa, Optimum skewed redundant inertial navigators, AIAA J. 12 (7) (1973) 899–902.
[10] S. Sukkarieh, P. Gibbens, B. Grocholsky, K. Willis, H. Durrant Whyte, A low-cost, redundant inertial measurement unit for unmanned air vehicles, Int. J. Robot. Res. 19 (11) (2000) 1089–1103.